# Aerogel Synthesis of Yttria-Stabilized Zirconia by a Non-Alkoxide Sol−Gel Route

Christopher N. Chervin,[†,‡] Brady J. Clapsaddle,[§] Hsiang Wei Chiu,[†] Alexander E. Gash,[§] Joe H. Satcher, Jr.,[§] and Susan M. Kauzlarich*[,†]

*Department of Chemistry, University of California at Davis, One Shields Avenue, Davis, California 95616, Lawrence Livermore National Laboratory, University Outreach, Livermore, California 94550, and Lawrence Livermore National Laboratory, Chemistry and Materials Science Directorate, Livermore, California 94550*

*Received February 17, 2005. Revised Manuscript Received April 15, 2005*

Homogeneous, nanocrystalline powders of yttria-stabilized zirconia (YSZ) were prepared using a non-alkoxide sol−gel method. Monolithic gels, free of precipitation, were prepared by addition of propylene oxide to aqueous solutions of $Zr^{4+}$ and $Y^{3+}$ chlorides at room temperature. The gels were dried with supercritical $CO_2(l)$, resulting in amorphous aerogels that crystallized into stabilized $ZrO_2$ following calcination at 500 °C. The aerogels and resulting crystalline products were characterized using in situ temperature profile X-ray diffraction, Raman spectroscopy, thermal analysis, transmission electron microscopy (TEM), scanning electron microscopy (SEM), nitrogen adsorption/desorption analysis, and elemental analysis by inductively coupled plasma-atomic emission spectroscopy. TEM and $N_2$ adsorption/desorption analysis of an aerogel prepared by this method indicated a porous network structure with a high surface area (409 $m^2/g$). The crystallized YSZ maintained high surface area (159 $m^2/g$) upon formation of homogeneous, nanoparticles (∼10 nm). Ionic conductivity at 1000 °C of sintered YSZ (1500 °C, 3 h) was $0.13 \pm 0.02\ \Omega^{-1}\ cm^{-1}$. Activation energies for the conduction processes from 1000 to 550 °C and 550−400 °C were $0.95 \pm 0.09$ and $1.12 \pm 0.05$ eV, respectively.

## Introduction

Yttria-stabilized zirconia (YSZ), a high-temperature oxide conductor, is a technologically significant material that finds extensive use as a solid-state electrolyte in applications such as solid oxide fuel cells and oxygen sensors.[1] YSZ has also been considered a good candidate for the oxide-conducting component of mixed ionic-electronic conducting composite electrodes and oxygen separation membranes.[2,3] Zirconia, the parent lattice in YSZ, is a polymorphic oxide that is monoclinic at room temperature and transforms to tetragonal and cubic phases at approximately 1443 and 2643 K, respectively.[4] The high-temperature phases, important for structural and oxide conduction applications, can be stabilized at room temperature through substitution of $Zr^{4+}$ with rare earth or alkali earth cations.[1] Charge compensation is balanced by the formation of oxygen vacancies which are necessary for thermally activated conduction processes.

For the case of $Y_2O_3$ substitution, cubic stabilization occurs above 8 mol % $Y_2O_3$.[5−8] However, there is discrepancy in the literature as to the necessary $Y_2O_3$ concentration for fully cubic stabilization. For example, cubic YSZ has been reported for $Y_2O_3$ concentrations above 8 mol %,[5] above 8.5 mol %,[6] and between 9 and 10 mol %.[7,8] In part, the discrepancy is due to the difficulty in distinguishing the tetragonal and cubic phases near the cubic-tetragonal phase boundary.[7] Below the concentration necessary for fully cubic stabilization a mixture of tetragonal and cubic phases exist with varying ratios of tetragonal to cubic, depending on $Y_2O_3$ concentration.[6] The optimal ionic conductivity of YSZ occurs at ∼8 mol %,[9] and most practical electrolyte applications of YSZ use 8−10 mol % $Y_2O_3$,[2,10] which correspond to fully cubic or mixed tetragonal-cubic YSZ.

In addition to composition, particle size and size distribution of precursor powders are important factors to consider when fabricating electrolytes and composite electrodes with YSZ.[11,12] Homogeneous powders consisting of submicrome-

* To whom correspondence should be addressed.
† University of California at Davis.
‡ Lawrence Livermore National Laboratory, University Outreach.
§ Lawrence Livermore National Laboratory, Chemistry and Materials Science Directorate.

(1) Subbarao, E. C.; Maiti, H. S. *Solid State Ionics* **1984**, *11* (4), 317−338.
(2) Minh, N. Q. *J. Am. Ceram. Soc.* **1993**, *76* (3), 563−88.
(3) Ji, Y.; Kilner, J. A.; Carolan, M. F. *Solid State Ionics* **2005**, *176* (9−10), 937−943.
(4) Subbarao, E. C. In *Advances in Ceramics, Vol. 3, Science and Technology of Zirconia*; Heuer, A. H., Hobbs, L. W., Eds.; American Ceramic Society: Westerville, OH, 1981; pp 1−24.
(5) Duwez, P.; Brown, F. H., Jr.; Odell, F. *J. Electrochem. Soc.* **1951**, *98*, 356−362.
(6) Ingel, R. P.; Lewis, D., III *J. Am. Ceram. Soc.* **1986**, *69* (4), 325−332.
(7) Yashima, M.; Ohtake, K.; Kakihana, M.; Arashi, H.; Yoshimura, M. *J. Phys. Chem. Solids* **1996**, *57* (1), 17−24.
(8) Strickler, D. W.; Carlson, W. G. *J. Am. Ceram. Soc.* **1964**, *47*, 122−126.
(9) Dixon, J. M.; LaGrange, L. D.; Merten, U.; Miller, C. F.; Porter, J. T., II *J. Electrochem. Soc.* **1963**, *110*, 276−280.
(10) Singhal, S. C. *Proc.−Electrochem. Soc.* **1998**, 97−24 (Ionic and Mixed Conducting Ceramics), 125−136.
(11) Sasaki, K.; Wurth, J. P.; Gschwend, R.; Godickemeier, M.; Gauckler, L. J. *J. Electrochem. Soc.* **1996**, *143* (2), 530−543.
(12) Kim, J. D.; Kim, G. D.; Moon, J. W.; Lee, H. W.; Lee, K. T.; Kim, C. E. *Solid State Ionics* **2000**, *133* (1−2), 67−77.

10.1021/cm0503679 CCC: $30.25 
Published on Web 05/24/2005

**Scheme 1. General Reaction Scheme for the Epoxide Addition Sol-Gel Process**

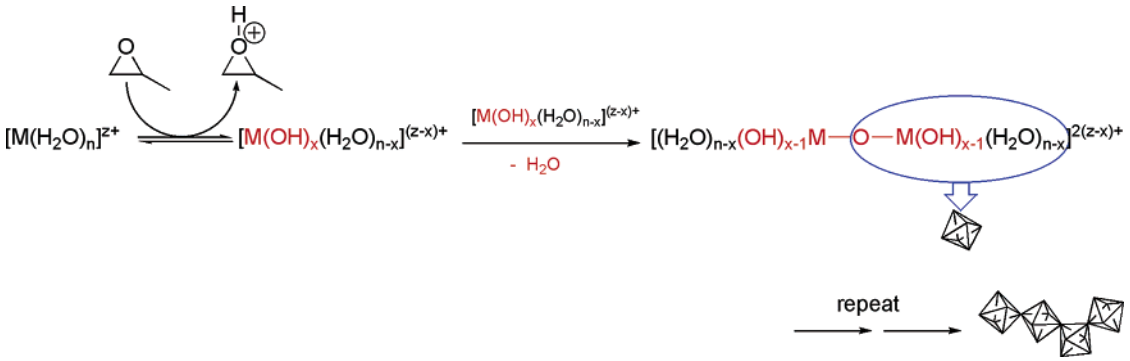


ter particles, free of hard agglomeration, can be beneficial for many fabrication techniques including slip-casting, tape casting, isostatic pressing, and colloidal spray deposition.[13,14] Nanoparticles have larger surface energies than micrometer-sized particles and, as a result, can potentially benefit ceramic processing by lowering sintering temperatures, increasing firing density, and creating nanosized grains in the fired ceramics.[13,15,16] Additionally, recent studies have demonstrated enhanced conductivity in nanocrystalline YSZ and other solid-state electrolytes.[14,17−19] Proposed mechanisms for the increased conductivity include dilution of impurities at the grain boundaries[17,19,20] and an increased number of defects due to the larger surface-to-bulk ratio of nanocrystalline materials.[19] Considering the demand for homogeneous, nanocrystalline YSZ powders in both commercial and laboratory applications, simple and effective preparation routes resulting in these morphologies are important and desirable.

Nanocrystalline YSZ has been prepared by various methods including sol−gel synthesis, spray pyrolysis, combustion synthesis, and coprecipitation routes.[21−23] Of these methods, sol−gel synthesis is a very common and exceptional technique because it provides a means of controlling the shape, morphology, and textural properties of the final materials.[24] The reported sol−gel techniques for preparing YSZ traditionally utilize alkoxide precursors and organic solvents.[25,26] These sol−gel techniques are either acid- or base-catalyzed and require the careful addition of water to prevent uncontrolled hydrolysis of Zr alkoxides.[24,27,28] Furthermore, atmospheric water leads to partial hydrolysis of the precursors, and often the reactions are carried out in nitrogen[29] or dehumidified atmospheres.[30] Chelating agents, such as acetylacetone, are sometimes added to help control hydrolysis during the gelation process.[31] Though these methods are sufficient for preparing nanocrystalline YSZ, simpler methods eliminating the need for alkoxide precursors and thereby the difficulties of handling the water-sensitive precursors, would be beneficial.

Recently, Gash and co-workers have reported an alkoxide-free, sol−gel synthesis technique for preparing various transition, main group, and rare earth metal oxides.[32−34] Through the use of an organic epoxide that acts as a proton scavenger, solutions of common hydrated metal salts undergo hydrolysis and condensation reactions to form metal oxide sol−gel materials, as shown in Scheme 1.[24,34−36] The "epoxide addition method" works well for several metal chloride and/or nitrate salts in water and other polar protic solvents (provided sufficient water is present), including both $Zr^{4+}$ and $Y^{3+}$ salts. This method eliminates the need for the often difficult preparation and handling of metal alkoxide precursors for nontraditional sol−gel metals and is complimentary to traditionally prepared sol−gel materials (i.e., $SiO_2$, $TiO_2$, $Al_2O_3$, etc.). Some examples of metal oxide gels prepared by the epoxide addition method include $Fe_2O_3$, $Cr_2O_3$, $Al_2O_3$, $Ga_2O_3$, and $ZrO_2$, and the method has also proven useful in the synthesis of a variety of binary metal-oxide systems.[33,37,38]

We report here a straightforward synthesis technique for the preparation of YSZ precursor sol−gels using the epoxide

(13) Mistler, R. E.; Twiname, E. R. *Tape casting: theory and practice*; American Ceramic Society: Westerville, OH, 2000.
(14) Xu, G.; Zhang, Y.-W.; Liao, C.-S.; Yan, C.-H. *Solid State Ionics* **2004**, *166* (3−4), 391−396.
(15) King, A. G. *Ceramic Technology and Processing*; William Andrew Publishing: New York, 2002.
(16) McColm, I. J. In *Ceramic Processing*; Terpstra, R. A., Pex, P. P. A. C., De Vries, A. H., Eds.; Chapman and Hall: New York, 1995; pp 1−8.
(17) Kosacki, I.; Anderson, H. U. *Ionics* **2000**, *6* (3 & 4), 294−311.
(18) Mondal, P.; Klein, A.; Jaegermann, W.; Hahn, H. *Solid State Ionics* **1999**, *118* (3, 4), 331−339.
(19) Tuller, H. L. *Solid State Ionics* **2000**, *131* (1, 2), 143−157.
(20) Kharton, V. V.; Marques, F. M. B. *Curr. Opin. Solid State Mater. Sci.* **2002**, *6* (3), 261−269.
(21) Gaudon, M.; Djurado, E.; Menzler, N. H. *Ceram. Int.* **2004**, *30* (8), 2295−2303.
(22) Jiang, S.; Schulze, W. A.; Amarakoon, V. R. W.; Stangle, G. C. *J. Mater. Res.* **1997**, *12* (9), 2374−2380.
(23) Ramamoorthy, R.; Sundararaman, D.; Ramasamy, S. *Solid State Ionics* **1999**, *123* (1−4), 271−278.
(24) Brinker, C. J.; Scherer, G. W. *Sol−Gel Science*; Academic Press: Boston, 1990.
(25) Ayral, A.; Assih, T.; Abenoza, M.; Phalippou, J.; Lecomte, A.; Dauger, A. *J. Mater. Sci.* **1990**, *25* (2B), 1268−1274.
(26) Okubo, T.; Nagamoto, H. *J. Mater. Sci.* **1995**, *30* (3), 749−757.
(27) Shukla, S.; Seal, S.; Vij, R.; Bandyopadhyay, S. *Nano Lett.* **2003**, *3* (3), 397−401.
(28) Wolf, C.; Ruessel, C. *J. Mater. Sci.* **1992**, *27* (14), 3749−3755.
(29) Okubo, T.; Takahashi, T.; Sadakata, M.; Nagamoto, H. *J. Membr. Sci.* **1996**, *118* (2), 151−157.
(30) Xia, C.; Cao, H.; Wang, H.; Yang, P.; Meng, G.; Peng, D. *J. Membr. Sci.* **1999**, *162* (1−2), 181−188.
(31) Debsikdar, J. C. *J. Non-Cryst. Solids* **1986**, *86* (1−2), 231−40.
(32) Gash, A. E.; Satcher, J. H., Jr.; Simpson, R. L. *Chem. Mater.* **2003**, *15* (17), 3268−3275.
(33) Gash, A. E.; Tillotson, T. M.; Satcher, J. H., Jr.; Hrubesh, L. W.; Simpson, R. L. *J. Non-Cryst. Solids* **2001**, *285* (1−3), 22−28.
(34) Gash, A. E.; Tillotson, T. M.; Satcher, J. H., Jr.; Poco, J. F.; Hrubesh, L. W.; Simpson, R. L. *Chem.* Mater. **2001**, *13* (3), 999−1007.
(35) Cotton, F. A.; Wilkinson, G. *Advanced Inorganic Chemistry*, 5th ed.; John Wiley and Sons: New York, 1988.
(36) Livage, J.; Henry, M.; Sanchez, C. *Prog. Solid State Chem.* **1988**, *18* (4), 259−341.

addition method. Monolithic gels are easily formed from $ZrCl_4$ and $YCl_3 \cdot 6H_2O$, using propylene oxide in distilled water. The gels are prepared in ambient atmosphere and temperature without elaborate or complicated synthetic equipment. The resultant wet gels are converted to aerogels by supercritical drying in $CO_2$ or to xerogels by slow drying in ambient atmosphere. Remarkably, the aerogel materials are observed to maintain a nanostructure following heat treatment at temperatures as high as 1000 °C, resulting in homogeneous, nanocrystalline powders of YSZ that can be further processed into a variety of forms (e.g., ceramics, thin films, etc). Aerogel processing has been reported for pure zirconia sol−gels prepared from traditional alkoxide methods;[39,40] however, to our knowledge, this is the first reported aerogel method for the preparation of YSZ. The YSZ powders prepared from this technique demonstrated bulk ionic conductivity consistent with literature-reported values.

## Experimental Section

**Synthesis of YSZ Nanoparticles.** YSZ-precursor gels containing 9 mol % $Y_2O_3$ were prepared by the epoxide addition method followed by supercritical drying in $CO_2(l)$. Anhydrous $ZrCl_4$ (99.9+%, Aldrich), $YCl_3 \cdot 6H_2O$ (99.9%, Aldrich), and propylene oxide (99%, Aldrich) were used as received. All gelation reactions were carried out at room temperature in ambient atmosphere. In a typical synthesis, $ZrCl_4$ (1.1652 g; 5 mmol) and $YCl_3 \cdot 6H_2O$ (0.3034; 1 mmol) were dissolved in distilled water (10 g; 555 mmol) such that the molar ratio of water to total metals was 93. Following complete dissolution of the salts, propylene oxide (PO; 3.2 g; 55 mmol) was added and briefly stirred (9:1 epoxide:metals molar ratio) to induce gelation. Clear monolithic gels, free of precipitates, resulted from all reactions.

Following gelation, the gels were aged for 24 h under ambient conditions in closed containers. The aged gels were then washed with ethanol for 3 days, with fresh ethanol exchanged daily. Wet gels were processed to aerogels by supercritical drying in a Polaron supercritical point drier. Ethanol in the wet gel pores was exchanged for $CO_2(l)$ for 2−3 days, after which the temperature of the vessel was ramped up to ∼45 °C, while a pressure of ∼100 bar was maintained. The vessel was then depressurized at a rate of ∼7 bar/h. Dried aerogels were calcined in air at 550 and 1000 °C using 2 °C /min ramps and 1 h dwell times.

**Physical Characterization.** Thermogravimetric analysis (TGA) and differential scanning calorimetry (DSC) of the resulting aerogels were performed simultaneously with a Netzsch 449 Thermal Analyzer in the temperature range of 25−1000 °C under flowing oxygen using a 10 °C/min ramp.

The crystallization of yttria-stabilized zirconia from the amorphous aerogels was monitored with in situ temperature profile X-ray diffraction using an Inel diffractometer operated at 30 A and 30 keV with Cu Kα radiation. The diffractometer was equipped with a furnace-heated sample holder and a position-sensitive detector allowing for diffraction measurements at selected temperatures during the calcination process. Diffraction data at each desired temperature was collected for 30 min. Room-temperature X-ray diffraction patterns of as-prepared and calcined aerogels were measured using a Scintag PAD V diffractometer operating at 40 A and 45 keV with Cu Kα radiation.

Raman spectroscopy of a YSZ aerogel calcined to 550 °C was measured to clarify the structure of the resultant crystalline material. Raman spectra from 100 to 800 $cm^{-1}$ were obtained at room temperature for a powdered sample using a Jobin Yvon Horiba HR 800 spectrometer. The Raman scattering was excited by a YAG laser source (wavelength of 532.0 nm) at 36 mW.

Surface area analysis was performed using an ASAP 2000 surface area analyzer (Micromeritics Instrument Corp.). Prior to analysis, samples of approximately 0.1−0.2 g were heated to 200 °C under vacuum ($10^{-5}$ Torr) for at least 24 h to remove adsorbed species. Nitrogen adsorption data were taken at five relative pressures from 0.05 to 0.20 at 77 K, and the surface area was calculated using BET (Brunauer−Emmett−Teller) theory.

Bright field transmission electron microscopy (TEM) analyses of an aerogel as-prepared and after calcination at 550 and 1000 °C were performed on a Philips CM-120 TEM, operating at 80 keV. TEM samples were prepared by dipping holey carbon-coated 400-mesh grids into methanol colloids of the respective powders, followed by drying at 120 °C overnight. Scanning electron microscopy was performed with a Philips 30XL FEG SEM operated between 5 and 10 keV. SEM samples were prepared by applying drops of methanol colloids of the respective powders on to hot aluminum SEM stubs, followed by drying at 120 °C overnight.

Elemental analysis of a YSZ aerogel calcined to 550 °C was determined by inductively coupled plasma-atomic emission spectroscopy (ICP-AES) performed by Galbraith Laboratories, Inc., of Knoxville, TN.

**Measurement of d.c. Ionic Conductivity of YSZ.** The ionic conductivity as a function of temperature for aerogel-derived YSZ powder was measured using the four probe d.c. technique of van der Pauw.[41] YSZ, calcined at 800 °C, was isostatically pressed into rectangular pellets at 930 bar and then sintered in air at 1500 °C for 3 h. YSZ powders were calcined prior to pressing to minimize weight loss during sintering and porosity in the final pellets. Platinum voltage and current electrodes were applied to the sintered pellets as a paste (Heraeus, CL11-5349) and fired at 900 °C for 30 min. The sintered pellets were approximately 1.75 cm in length and 0.1 $cm^2$ in cross-section, and the voltage electrode separation was 0.8 cm. Platinum wires were attached to the electrodes with Pt paste followed by an additional sintering at 900 °C for 30 min. The instrument leads were connected to the platinum wires and the samples were placed in quartz tubes.

Conductivity measurements were made in tube furnaces under flowing air (1 L/min) from 1000 to 400 °C at 50 or 100 °C intervals, depending on the temperature range. For each temperature a constant current was applied with a Solartron SI 1287 Electrochemical Interface and the steady-state voltage was measured. Currents ranged from 0.01 A to 1 μA, depending on sample resistivity.

## Results and Discussion

**Synthesis.** Addition of PO to aqueous solutions containing $Zr^{4+}$ and $Y^{3+}$ chlorides resulted in the formation of clear monolithic gels free of precipitates. The gelation time ($t_{gel}$) was rapid, on the order of minutes, and varied with the molar ratio of PO to total metals, $R_{epox}$. For a constant volume of water and $R_{epox} = 5$, 7, and 9, the $t_{gel}$'s were 4.5, 1.5, and 0.5 min, respectively. The $t_{gel}$'s were qualitatively determined as the elapsed time between addition of PO and the point at

(37) Clapsaddle, B. J.; Gash, A. E.; Satcher, J. H.; Simpson, R. L. *J. Non-Cryst. Solids* **2003**, *331* (1−3), 190−201.
(38) Clapsaddle, B. J.; S., D. W.; Gash, A. E.; Satcher, J. H., Jr.; Simpson, R. L. *J. Non-Cryst. Solids* **2004**, in press.
(39) Bedilo, A. F.; Klabunde, K. J. *Nanostruct. Mater.* **1997**, *8* (2), 119−135.
(40) Ward, D. A.; Ko, E. I. *Chem. Mater.* **1993**, *5* (7), 956−969.
(41) Van der Pauw, L. J. *Philips Res. Rep.* **1958**, *13*, 1−9.

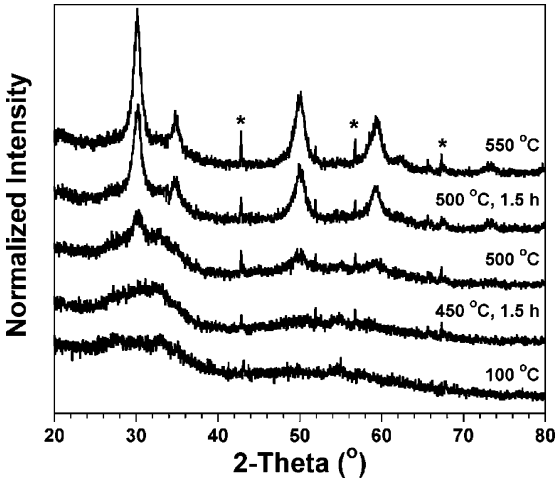


**Figure 1.** In situ temperature profile XRD of a YSZ aerogel. Diffraction patterns were measured immediately after reaching each temperature and once again after dwelling for 1.5 h. Only selected diffraction profiles are shown to prevent redundancy. Additional peaks associated with the $Al_2O_3$ sample holder become apparent during shrinkage of the sample during heating. The sharp $Al_2O_3$ peaks are easily distinguished from the broad (nanocrystalline) YSZ phase and are marked with an *.

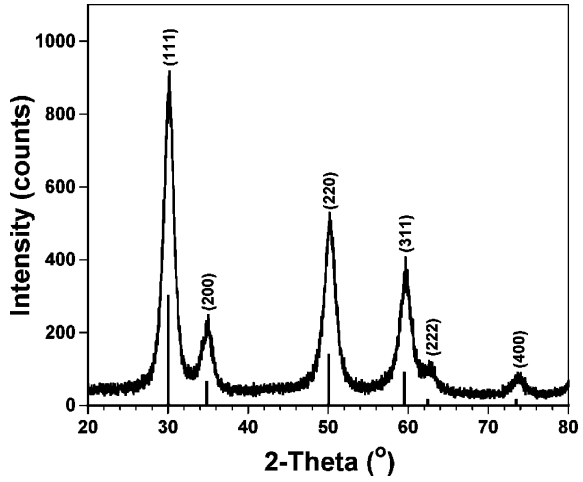


**Figure 2.** Room-temperature XRD pattern of a YSZ aerogel calcined at 550 °C. Peak positions from PDF Card # 82-1246 (cubic yttria-stabilized zirconia) are marked with sharp lines.

which the sols no longer flowed under the influence of gravity when the reaction containers were tilted. The gelation points were generally preceded by notable changes in the solution viscosity and a slight degree of opacity.

Supercritical drying of the wet gels resulted in partially monolithic aerogels, which were easily ground into powders. The ultrafine, homogeneous powders had nanoparticulate morphologies, were X-ray amorphous, and upon calcination crystallized into yttria-stabilized zirconia. The variation of $R_{epox}$ during the initial wet-gel synthesis did not appear to have any affect on the final calcined powder morphology or diffraction patterns. For simplicity, the as-prepared aerogels will be referred to as YSZ-aerogels but technically speaking they were amorphous until after calcination.

The Zr/Y ratio of a YSZ aerogel ($R_{epox} = 7$) calcined to 550 °C, as determined by ICP-AES, was 4.89, corresponding to 9.49 mol % YSZ. The expected ratio and mol % from the synthesis were 5.13 and 9.09 mol %, respectively. Therefore, the amount of $Y^{3+}$ incorporated into the gel was higher than expected, suggesting that some $Zr^{4+}$ was removed during the washing step or did not react completely during the gelation process. Several factors may affect the incorporation of multiple cations into a single gel using the epoxide addition method, such as the reaction kinetics of the cation precursors, cation concentration and solubility, epoxide type and concentration, and solvent type. The expected and resultant Zr/Y ratio in YSZ prepared over a range of mol % are currently under investigation.

**Powder X-ray Diffraction.** Figure 1 shows in situ temperature profile powder XRD patterns of a YSZ aerogel prepared with $R_{epox} = 9$. The diffraction patterns were measured immediately after reaching the desired temperature and once again after dwelling at the specific temperature for 1.5 h. The YSZ-aerogel was X-ray amorphous up to 450 °C. Crystallization had partially occurred by 500 °C and crystallinity increased with prolonged calcination at that temperature. Further calcination to 550 °C did not significantly alter the diffraction pattern. Room-temperature XRD of the sample following heat treatment at 550 °C is shown in Figure 2. The significant amount of peak broadening observed is due to the nanocrystalline nature of the calcined aerogel. The peak positions are in agreement with the reported reflections for cubic zirconia (PDF Card # 82-1246). However, due to peak broadening and the similar peak positions for tetragonal $ZrO_2$, the diffraction pattern could also be indexed as tetragonal (PDF card # 82-1245). Therefore, Raman spectroscopy was used to further elucidate the structure type.

**Raman Spectroscopy.** The cubic to tetragonal phase transition in doped zirconia occurs by both elongation of one of the crystallographic axes relative to the other two[42] and displacement of oxygen from the ideal anion site in the fluorite structure.[43] The relatively small atomic scattering factor of oxygen makes it difficult to distinguish between the cubic and tetragonal phases near the phase boundary (8−10 mol % $Y_2O_3$) with XRD. However, Raman spectroscopy is sensitive to polarizability of the oxygen ions and therefore can be used to determine the symmetry of YSZ.[44] The Raman spectrum for cubic YSZ is characterized by a broad peak near 530−670 $cm^{-1}$ and additional poorly defined structures related to the disordered oxygen sublattice.[45,46] Spectrum for the tetragonal phase, however, is characterized by six relatively sharp peaks at approximately 115, 266, 326, 474, 616, and 646 $cm^{-1}$.[44]

Raman spectrum for the calcined aerogel analyzed with ICP-AES (9.49 mol %) is shown in Figure 3. The material is predominantly cubic with a broad peak observed between 575 and 640 $cm^{-1}$ and having a maximum at 620 $cm^{-1}$. The relatively distinct peaks associated with the tetragonal phase are not observed; however, weak, broad structures are noted at 256 and 328 $cm^{-1}$, suggesting that trace amounts of tetragonal phase may be present. This is consistent with

(42) LeFevre, J.; Collongues, R.; Perez, Y.; Jorba, M. *C. R. Acad. Sci.* **1959**, *249*, 2329−2331.
(43) Teufer, G. *Acta Crystallogr.* **1962**, *15*, 1187.
(44) Feinberg, A.; Perry, C. H. *J. Phys. Chem. Solids* **1981**, *42* (6), 513−518.
(45) Keramidas, V. G.; White, W. B. *J. Phys. Chem. Solids* **1973**, *34*, 1873.
(46) Kontoyannis, C. G.; Orkoula, M. *J. Mater. Sci.* **1994**, *29* (20), 5316−5320.

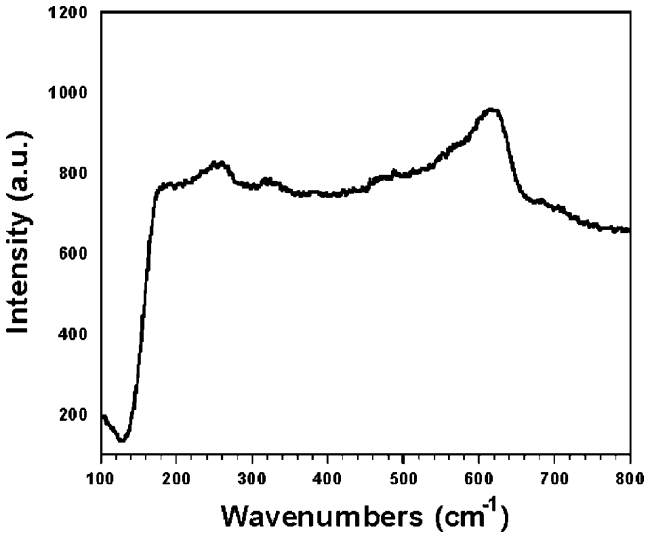


**Figure 3.** Raman spectroscopy of a YSZ aerogel calcined to 550 °C (9.49 mol % $Y_2O_3$). The broad peak with maximum at 620 $cm^{-1}$ indicates the cubic symmetry of the material.

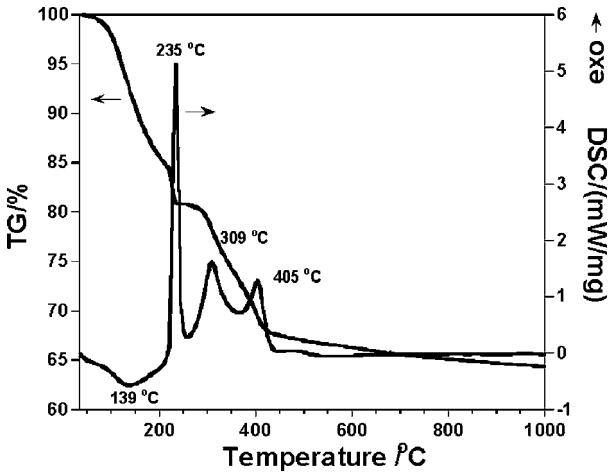


**Figure 4.** Simultaneous TGA/DSC scans of a dried YSZ aerogel, $R_{epox} = 9$ (10 °C/min ramp under flowing oxygen).

results by Yashimia et al., who found the cubic-tetragonal phase boundary between 9 and 10 mol % $Y_2O_3$.[7]

**Thermal Analysis.** Figure 4 shows the simultaneous TGA/DSC traces under flowing oxygen for an aerogel prepared with $R_{epox} = 9$. Several major peaks are observed in the DSC curve and each corresponds to weight loss measured by TGA. The first peak is a broad endotherm with a minimum at 139 °C that is attributed to the combined loss of water and residual organics from the gel preparation. This peak occurs concurrently with a TGA weight loss of 16%. The second DSC peak, a sharp exotherm with a maximum at 235 °C, may be due to oxidation of residual organic compounds and corresponds to a sharp weight loss of 3%. Two additional exotherms occur with maxima at 309 and 405 °C and a combined weight loss of 13%. The total mass loss for the gel heated to 1000 °C, as determined by TGA, was 36%, the majority of which occurred below 400 °C (30%). The remaining 6% weight loss above 400 °C is likely due to elimination of water as chemisorbed hydroxyl groups react to form additional M−O−M bonds.[47]

A distinct exotherm related to crystallization was not observed in the DSC data; however, a small, broad exothermic feature is discernible from 450 to 500 °C. Based on XRD results (Figures 1 and 2), the crystallization of YSZ was expected to occur above 450 °C with the phase transition only partially occurring upon reaching 500 °C. Prolonged calcination at that temperature was required to complete formation of a highly nanocrystalline phase. Considering the DSC heating rate of 10 °C/min, it is not unexpected to find a broad exotherm as opposed to a sharp crystallization peak. The observed three exotherms at temperatures below 450 °C correspond closely with sharp weight losses and amorphous XRD structures, and therefore are attributed to the oxidation of residual organic components or formation of M−O−M bonds through condensation and elimination of $H_2O$.

**Electron Microscopy.** Brightfield TEM images confirm that the YSZ-aerogels crystallize into powders that remain nano-particulate even after high-temperature calcination. Micrographs of a YSZ-aerogel and samples calcined at 550 and 1000 °C are shown in Figure 5. An extended nanoparticulate network resulted during the sol−gel processing of the YSZ-aerogel (Figure 5a). Following calcination at 550 °C, individual YSZ particles are distinguishable with diameters under 10 nm (Figure 5b). After calcination at 1000 °C, particle sizes increased to 30−40 nm, but without any further change in morphology (Figure 5c). These results indicate that the extended network of the original YSZ-aerogel is no longer present after calcination, but instead crystalline powders of nanometer-sized particles with narrow size distributions are obtained. SEM images of the powder calcined at 550 and 1000 °C, shown in Figure 6, further confirm the homogeneous, nanoscopic nature of the YSZ. In addition, SEM analysis reveals no evidence of hard agglomeration in the final powders.

**Surface Area Analysis.** The surface area of the porous networked YSZ-aerogel (Figure 5a) was 406 $m^2/g$. Following calcination at 550 and 1000 °C, the YSZ surface areas were 159 and 26.0 $m^2/g$, respectively. With use of the experimentally determined surface areas and the assumption that all particles are spherical, the average particle size ($d_{BET}$) can be calculated for the powders using

$$d_{BET} = 6/(\rho S_v) \quad (1)$$

where $\rho$ is the materials density and $S_v$ the specific surface area of the sample. With use of the theoretical density of 5.9503 $g/cm^3$ for 9 mol % $Y_2O_3$-stabilized $ZrO_2$,[6] the calculated $d_{BET}$ for the aerogels calcined at 550 and 1000 °C were 6.3 and 39 nm, respectively, in good agreement with the TEM data. The average particle size for the YSZ-aerogel was not calculated because the density of the amorphous oxide is unknown. In addition, the TEM data indicate that the amorphous particles exist in extended porous networks and are not spherical in nature.

**Gel Structure.** In this study gelation occurred in a homogeneous fashion from the precursor solution, which suggests the extended network that formed contained uniformly mixed $Y^{3+}$ and $Zr^{4+}$ oxo-species.[36] The actual composition of the YSZ-aerogel is unknown, but certainly

(47) Hench, L. L.; West, J. K. *Chem. Rev.* **1990**, *90* (1), 33−72.

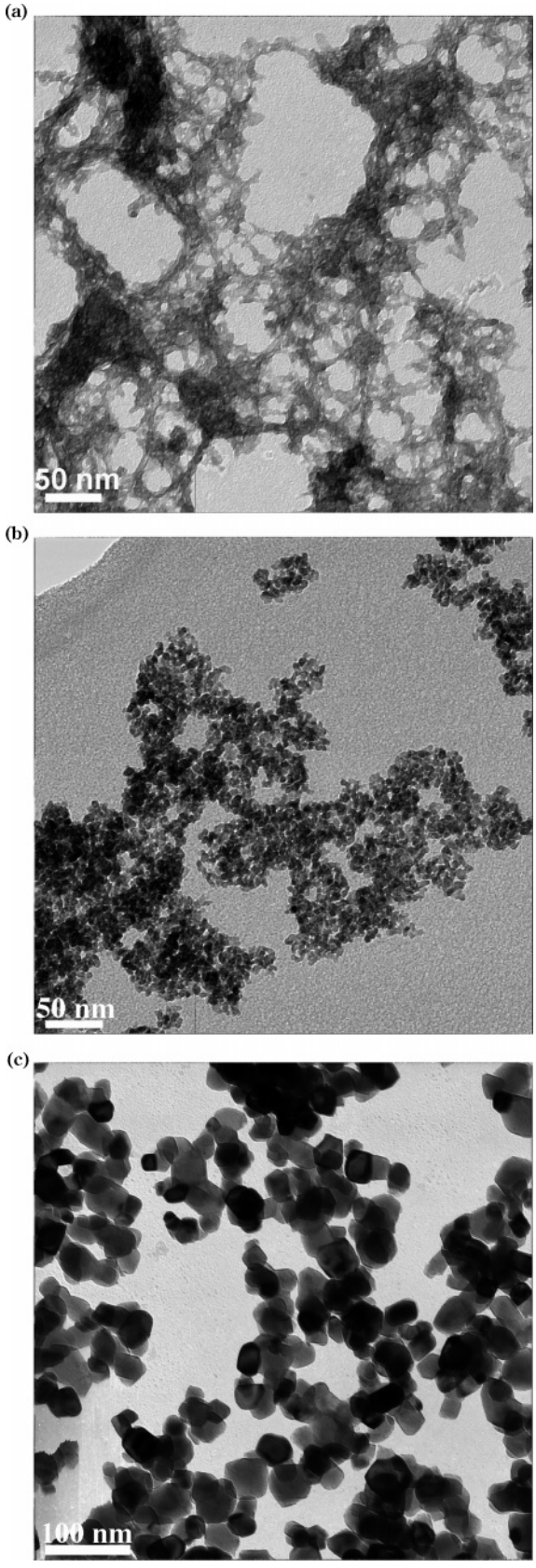


**Figure 5.** Bright field TEM micrographs of a YSZ aerogel, $R_{epoxide} = 9$: (a) as-prepared, (b) calcined at 550 °C, and (c) calcined at 1000 °C.

contains a high degree of hydroxyl groups, as is evidenced from the significant weight loss during calcination. Uniform mixing of $Y^{3+}$ and $Zr^{4+}$ is apparent by in situ XRD data, revealing crystallization of yttria-stabilized zirconia at low temperature without intermediate oxide formation. Furthermore, TEM and SEM demonstrate the oxide is extremely homogeneous. Extended binary oxide networks that were formed during the sol−gel process are inherently mixed on the atomic level, which is a key advantage over conventional solid-state synthesis techniques.

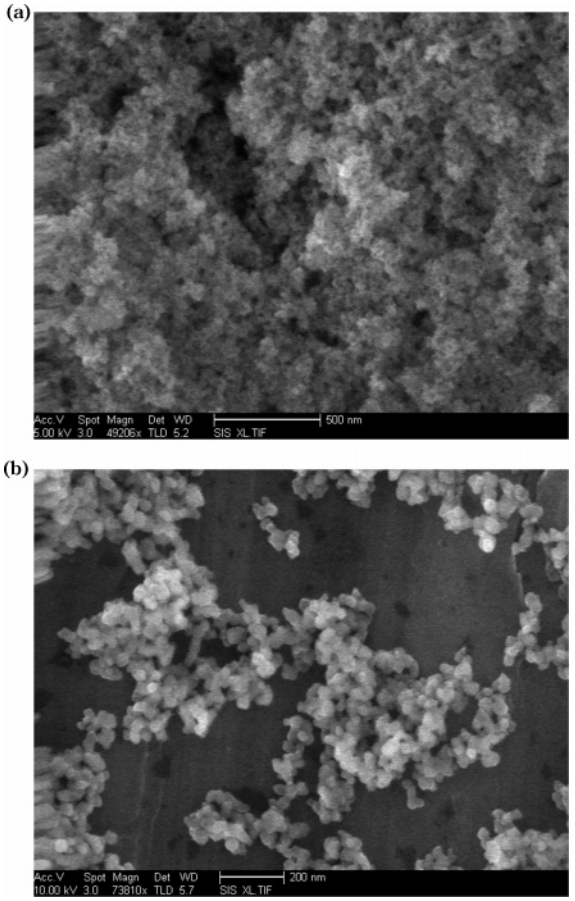


**Figure 6.** SEM images of a YSZ aerogel calcined at (a) 550 °C and (b) 1000 °C.

The monolithic sol−gels were sensitive to the drying step and resulted in significantly different morphologies depending on the drying method. Supercritical drying (aerogels) produced fluffy, soft materials, whereas drying under ambient conditions (xerogels) resulted in very coarse materials that were difficult to grind to fine powder. Furthermore, when using xerogel starting materials, hard agglomerates were obtained upon calcination as opposed to the distinct nanoparticles obtained from the aerogel starting materials. The difference in morphology, crystallinity, surface area, and particle agglomeration between xerogel and aerogel processed gels are currently under investigation.

**Ionic Conductivity.** Electrical resistivity of YSZ is measured as a function of temperature and in general reported as conductivity ($\sigma$)

$$\sigma = 1/R \tag{2}$$

where $R$ is the bulk resistivity of the material. The temperature dependence of YSZ can be expressed as

$$\sigma(T) = A/T \exp(-E_a/kt) \tag{3}$$

where $E_a$ is the activation energy, $k$ is the Boltzmann

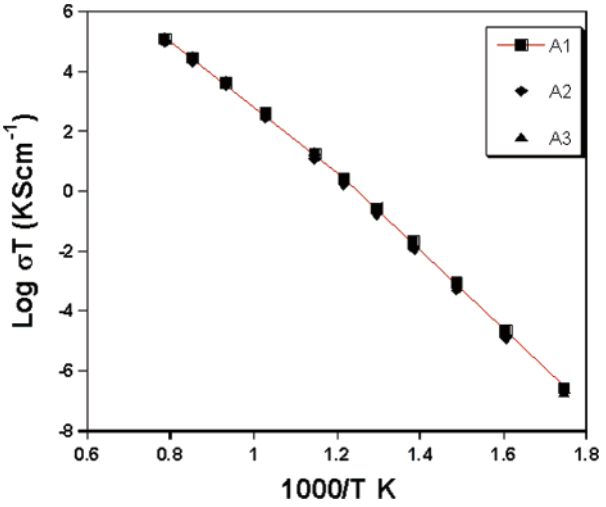


**Figure 7.** Plot of ln($\sigma T$) as a function of $10^4$/T for sintered YSZ pellets prepared from aerogel powders.

**Table 1. Activation Energy and Conductivity Results for Sintered YSZ Aerogels**

| sample | $E_a$ > 550 °C (eV) | $E_a$ < 550 °C (eV) | $\sigma$ at 800 °C ($\Omega^{-1}$ cm$^{-1}$) | $\sigma$ at 1000 °C ($\Omega^{-1}$ cm$^{-1}$) |
|---|---|---|---|---|
| A1 | 0.96 ± 0.06 | 1.12 ± 0.03 | 0.032 ± 0.004 | 0.12 ± 0.02 |
| A2 | 0.95 ± 0.06 | 1.13 ± 0.03 | 0.039 ± 0.001 | 0.140 ± 0.004 |
| A3 | 0.94 ± 0.06 | 1.10 ± 0.03 | 0.036 ± 0.002 | 0.130 ± 0.006 |

constant, and $A$ is the pre-exponential factor.[48] The activation energy for the conduction process is obtained from the slope of a plot of ln($\sigma T$) versus 1/$T$.

Figure 7 shows ln($\sigma T$) as a function of $10^4/T$ plotted for three sintered YSZ pellets prepared from calcined aerogel powders. The geometric density of the pellets, which are labeled A1, A2, and A3, were 95.2, 94.9, and 96.8% of theoretical,[6] respectively. The data show a change in slope around 550 °C toward lower activation energy at higher temperature, in agreement with previously reported results for YSZ.[49,50] The activation energies, determined separately for the two temperature regions of 400−550 °C and 550−1000 °C, are listed in Table 1. Also listed in Table 1 are the bulk ionic conductivities for each sample at 1000 and 800 °C, both common operating temperatures for solid oxide fuel cells utilizing YSZ components.

The ionic conductivities for the sintered YSZ aerogel at 800 and 1000 °C were 0.036 ± 0.005 and 0.13 ± 0.02 $\Omega^{-1}$ cm$^{-1}$, respectively. These are in good agreement with accepted values for total conductivity of 9 mol % YSZ at the respective temperatures.[1,51] The activation energies for the high- and low-temperature regions were 0.95 ± 0.09 and 1.12 ± 0.05 eV, respectively. These results, within experimental error, are in agreement with work by Petot et al. for the activation energies in single-crystal 9 mol % YSZ, which were found to be 0.93 ± 0.03 and 1.08 ± 0.03 for the high- and low-temperature regions, respectively.[50]

The 4-probe, d.c. method is used to obtain total resistivity, which for YSZ is composed of bulk and grain boundary contributions.[49] In this study we have measured total resistivity of YSZ sintered at high temperature (1500 °C) to demonstrate the materials suitability as an oxide conductor for electrolyte and composite cathode applications. The objective was to study the bulk conductivity and, therefore, high sintering temperatures in which the grain sizes are expected to be on the order of micronmeters were used. We are currently investigating the effects of these high surface area, nanocrystalline YSZ powders in porous SOFC composite cathode applications. Potentially, aerogel-derived YSZ will provide reduced sintering temperature, larger surface area, and improved reaction kinetics of the porous cathodes.

## Conclusions

The epoxide addition sol−gel method was successfully applied to the synthesis of 9 mol % yttria-stabilized zirconia. This technique provides a straightforward method for the preparation of homogeneous YSZ precursor gels in aqueous solution without the need for alkoxide precursors or elaborate reaction schemes. Supercritical drying of the wet gels produced ultrafine, homogeneous powders with nanoparticulate morphologies. The amorphous aerogels crystallized into YSZ at approximately 500 °C while maintaining a high surface area and particle diameters below 10 nm. Raman spectroscopy of a calcined aerogel (9.49 mol % $Y_2O_3$) indicated it was predominantly cubic with trace amounts of tetragonal symmetry, suggesting the material was very near the cubic-tetragonal phase boundary. Conductivity measurements of sintered YSZ aerogels were in excellent agreement with previously reported data for YSZ. The materials prepared by this method are currently being evaluated for potential use in solid oxide fuel cell composite cathodes.

**Acknowledgment.** This work was supported by the University of California Energy Institute, the National Science Foundation (Grant DMR-0120990), and the Department of Energy (Student Employee Graduate Research Fellowship). The authors thank Julie Muyco, for Raman spectroscopy measurements, Alexandra Navrotsky, for use of the Scintag X-ray diffractometer and TGA/DSC, and David W. Sprehn for technical support. This work was performed under the auspices of the U.S. Department of Energy by the University of California, Lawrence Livermore National Laboratory, under Contract No. W-7405-Eng-48.

CM0503679

(48) Strickler, D. W.; Carlson, W. G. *J. Am. Ceram. Soc.* **1965**, *48* (6), 286−289.
(49) Badwal, S. P. S. *J. Mater. Sci.* **1984**, *19* (6), 1767−1776.
(50) Petot, C.; Filal, M.; Rizea, A. D.; Westmacott, K. H.; Laval, J. Y.; Lacour, C.; Ollitrault, R. *J. Eur. Ceram. Soc.* **1998**, *18* (10), 1419−1428.
(51) Etsell, T. H.; Flengas, S. N. *Chem. Rev.* **1970**, *70* (3), 339−376.